FerriNaphth: A fluorescent chemodosimeter for redox active metal ions†

Randy K. Jackson, Yu Shi, Xudong Yao and Shawn C. Burdette*

Received 11th January 2010, Accepted 15th February 2010
First published as an Advance Article on the web 23rd March 2010
DOI: 10.1039/c000248h

FerriNaphth, a fluorescent chemodosimeter for Fe^{III}, has been prepared and characterized. The probe consists of a catechol ligand linked to a naphthalimide fluorophore by an aniline nitrogen linker. Upon exposure to Fe^{III}, the aminocatechol of FerriNaphth is oxidized to the corresponding quinone, which in its imine-one tautomer, is hydrolyzed to liberate a fluorescent aminonaphthalimide derivative. The fluorescence behavior is consistent with oxidation being promoted by metal coordination.

Introduction

Fluorescent probes for metal ions like Ca^{II} and Zn^{II} have become widespread in biological imaging because of their unique ability to quantify changes in the temporal and spatial concentrations of these analytes passively.[1,2] The design of probes that exhibit fluorescent enhancement upon exposure to $Fe^{II/III}$ and $Cu^{I/II}$ remains a significant challenge because redox active metal ions provide multiple non-radiative decay pathways for the excited states of fluorophores. As a result, probes that show fluorescence enhancement upon interaction with transition metal ions remain scarce.[3,4] Recently, we reported the design and synthesis of a fluorescent probe for redox active metal ions to begin addressing this problem.[5] In FerriBRIGHT, Fe^{III} and Cu^{II} oxidize a catechol appended to a BODIPY fluorophore into a quinone. The oxidation of the catechol interrupts photoinduced electron transfer (PeT) quenching of the fluorophore, which enhances the intensity of the probe's emission. In addition to our system, a reversible quinone/hydroquinone switch was used to construct a redox probe, which further demonstrates the ability to use the redox behaviour of a tethered substrate to elicit a fluorescence response.[6] The design element consists of a 1,4-quinone coupled to a BODIPY fluorophore *via* a phenylene spacer. The BODIPY-quinone dyad fluoresces weakly owing to PeT from the quinone moiety to the fluorophore. After exposure to a reducing agent, however, fluorescence increases because formation of the corresponding hydroquinone interrupts the PeT process. Additional fluorescent probes for biological oxidants have been reported that use similar BODIPY-quinone systems.[7,8]

Many probes for redox active species possess the characteristics of chemodosimeters, since the fluorescence response is irreversible. While several strategies for constructing chemodosimeters for Fe^{III} and Cu^{II} have been demonstrated,[9-11] the majority utilize transition metal-induced ring opening of a weakly fluorescent spirolactam compound.[12-14] These probes integrate a fluorescent reporting group with an analyte recognition moiety linked covalently to the spirolactam amide nitrogen atom. Metal coordination mediates the ring opening reaction that generates the emissive isomer of the fluorophore.

Sensors that emit at a different wavelength in the apo and bound forms possess advantages in biological imaging applications. Ratiometric sensors often involve internal charge transfer (ICT) to induce wavelength shifts. Several naphthalimide derived sensors for Cu^{II} take advantage of ICT to shift absorption and emission wavelengths,[15-18] suggesting that dyads comprised of these fluorophores and metal-binding ligands are good candidates for fluorescent probes. We hypothesized that oxidizing a catechol ligand conjugated to a naphthalimide fluorophore would result in an ICT state that would shift the absorption and emission wavelengths sufficiently to efficiently detect Fe^{III}. Naphthalimide fluorophores are prototypical donor–acceptor systems, where conjugating an electron pair donor with one of the imide carbonyls leads to the maximum fluorescence output.[19] We reasoned that an aniline nitrogen linker would be the best candidate to couple the naphthalimide with the catechol because it would be conjugated to both the fluorophore and the metal receptor (Fig. 1).

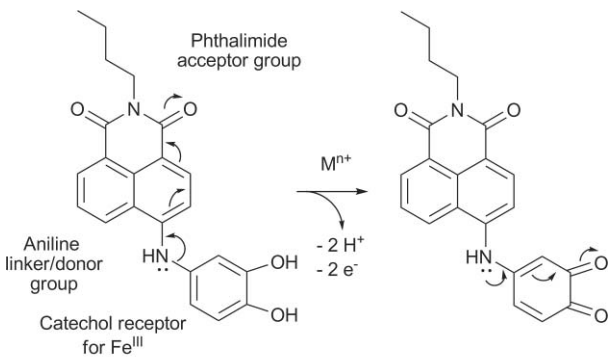

Fig. 1 Design and signalling mechanism of FerriNaphth. In the absence of metal ions, the lone pair on the aniline nitrogen participates in a donor–acceptor resonance interaction with the phthalimide carbonyl group. After oxidation with Fe^{III}, the aniline also can engage in a resonance interaction with the quinone carbonyl, which would lead to different absorption and emission characteristics by an ICT mechanism.

Department of Chemistry, University of Connecticut, Storrs, CT 06269-3060, USA. E-mail: shawn.burdette@uconn.edu

† Electronic supplementary information (ESI) available: NMR spectra for new compounds. Absorption spectra for Cu^{II} oxidation of FerriNaphth in CH_3CN and CH_3OH. Absorption and emission spectra for Fe^{III} oxidation of FerriNaphth in CH_3OH. Absorption spectrum for the titration of FerriNaphth with Ga^{III}. Absorption spectrum of oxidized FerriNaphth at different concentrations and corresponding Beer's law plot. Absorption spectra in CH_3CN of various Fe^{III} and Cu^{II} salts used in these studies. See DOI: 10.1039/c000248h

Results and discussion

The desired fluorescent probe was prepared using a Pd-catalyzed aryl amination between 4-bromo-*N*-butyl-1,8-naphthalimide (**2**)[20] and 5-aminospiro(1,2-benzodioxole-2,1′cyclohexane) (**3**)[21] that provided the precursor ligand in 58% yield after purification by column chromatography (Scheme 1). Removal of the cyclohexylidene ketal with concentrated HCl provided FerriNaphth. The name FerriNaphth is derived from the fluorophore (naphthalimide) and the target analyte (ferric iron). FerriNaphth is a red crystalline solid that is soluble in organic solvents, but only sparingly soluble in aqueous solution. When dissolved in anhydrous acetonitrile, FerriNaphth absorbs with a λ_{max} at 441 nm ($\varepsilon = 16200\ cm^{-1}\ M^{-1}$) and displays weak emission with a λ_{max} at 520 nm ($\Phi = 0.001$). Upon exposure of FerriNaphth to $Fe(NO_3)_3$ the absorption peak at 441 nm erodes over a period of 3 min, with the concomitant formation of a new peak at 368 nm (Fig. 2, top). An increase in the emission intensity centered at 520 nm is observed after the addition of H_2O when excited at 400 nm (Fig. 2, bottom); however, no significant changes in emission behavior are observed under anhydrous conditions. Similar changes are observed in the absorption spectra when CH_3OH was used as a solvent; however, the changes in emission are less pronounced. Using the nitrate salt eliminates bands from $FeCl_3$ and $Fe(ClO_4)_3$ that overlap the absorption peaks of FerriNaphth, but has no significant impact on the fluorescence response. Absorption bands blue-shift in typical ICT-based naphthalimide sensors, but emission wavelengths do not red-shift.[22] Since the changes in the absorption spectra contradicted predicted ICT behavior, the product of iron oxidation was interrogated. Analysis of solutions containing the probe and Fe^{III} by TLC revealed the presence of a fluorescent compound and a bright red species that decomposed upon solvent removal. The fluorescent compound was isolated and identified as *N*-^{n}butyl-4-aminonaphthalimide (**7**).[19,23] The presence of **7** suggests that instead of an ICT system, the fluorescence signal transduction mechanism of FerriNaphth involves metal-promoted oxidation followed by a second chemical transformation.

Aminoxyquinones like **5** are tautomeric red compounds,[24] and investigations revealed that the addition of water and 10 mol% pyridyl *p*-toluenesulfonic acid accelerate the disappearance of the red species and increase the intensity of emission from **7**. These observations suggest that oxidized FerriNaphth, which

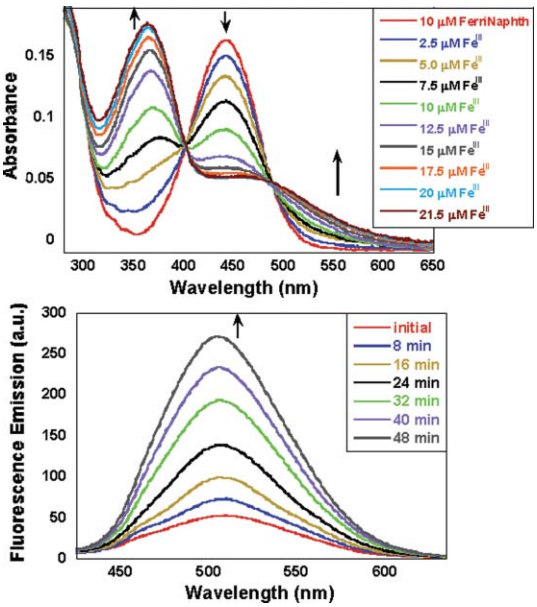

Fig. 2 Oxidation of 10 μM FerriNaphth in CH_3CN with incremental additions of $Fe(NO_3)_3$. Absorbance (top) measurements were recorded after no additional changes were observed after each addition. Emission spectra (bottom) were recorded over a period of 48 min after the addition of 2 equivalents of $Fe(NO_3)_3$ and 1% H_2O by volume. Excitation was provided at 400 nm with an excitation slit width of 5.0 nm and an emission slit width of 10 nm.

can exist in both a quinone (**5**) and an imine-one tautomer (**6**), subsequently undergoes imine hydrolysis to provide the fluorescent naphthalimide **7** (Scheme 2). In addition to this mechanistic evidence, a charge transfer band at 562 nm corresponding to the $[Fe(ferrozine)_3]^{4-}$ complex forms when FerriNaphth is oxidized by Fe^{III} in the presence of ferrozine, a common Fe^{II} indicator (Fig. 3). The catechol to quinone transformation requires a 2 electron oxidation, and the amount of ferrous iron present after the oxidation corresponds to approximately 2 equivalents of ferric iron reacting with every equivalent of FerriNaphth in solution.

Relatively few chemodosimeters have been designed where a turn-on fluorescence signal results from hydrolysis of the weakly fluorescent parent molecule.[25-29] Typically these probes exploit

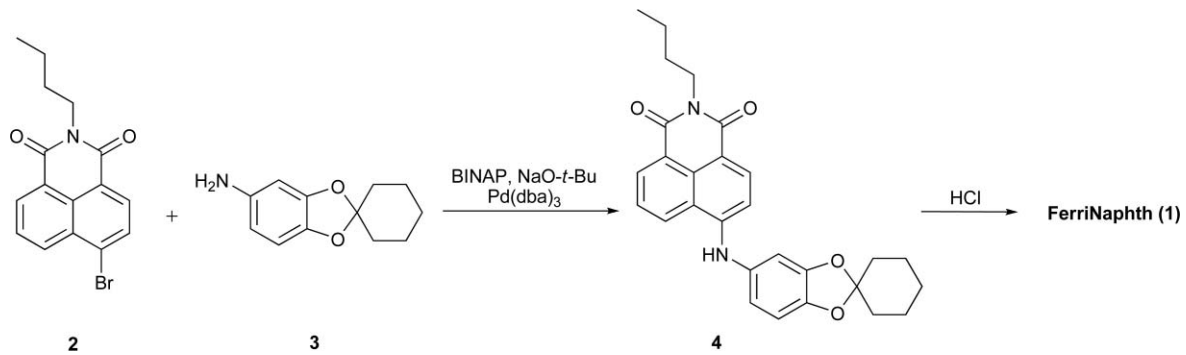

Scheme 1 Synthesis of FerriNaphth.

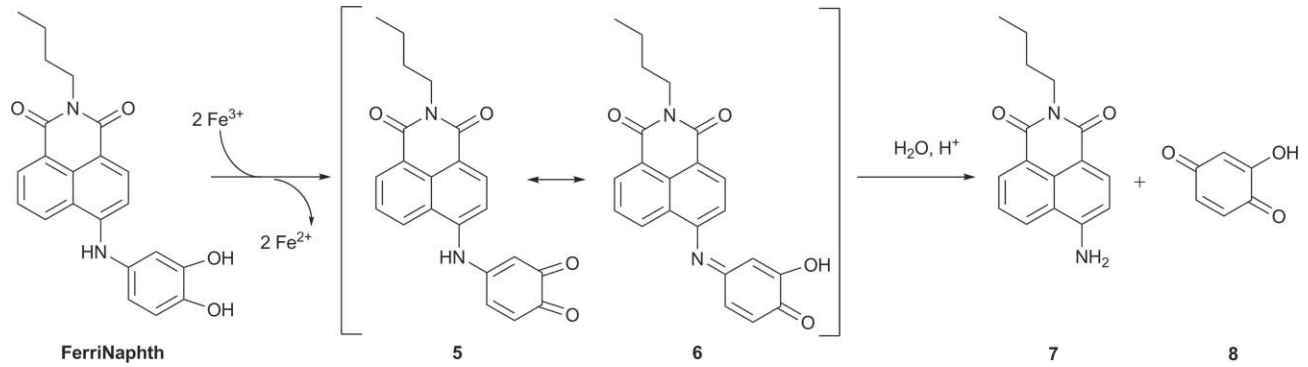

Scheme 2 Fluorescence transduction mechanism of FerriNaphth.

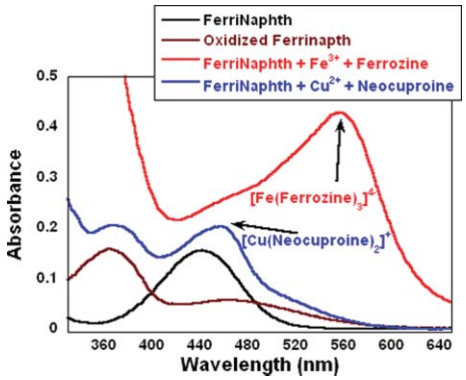

Fig. 3 Absorbance spectra of 10 μM FerriNaphth (CH_3CN) in the presence of 10 equivalents of Fe^{III} or Cu^{II} and with either 10 or 20 equivalents of ferrozine or neocuproine respectively.

the Lewis acidity of a metal ion to promote the liberation of a fluorophore that is quenched by the reactive bonding interactions. In a probe that selectively responds to Fe^{III}, Schiff bases from a chelating ligand hydrolyze to release a highly fluorescent coumarin fluorophore.[26] While other fluorescent chemodosimeters for Fe^{III} based on oxidation chemistry and fluorophore isomerization have been reported,[9-11] there has been only one report of a system utilizing both oxidation and hydrolysis to achieve an emission enhancement in the presence of a redox active transition metal.[10] In the squaramide hydroxamate system however, multiple products from the redox process were observed and only a few that were responsible for the emission enhancement were characterized successfully.

The emission intensity of **7** is polarity dependent, and has a quantum yield of 0.74 in CH_3CN.[19] Repeating the fluorescence assay in nonpolar solvents like THF and CH_2Cl_2 with 1% H_2O provides a more intense fluorescence signal. Experiments using protic solvents like H_2O and CH_3OH only result in weak emission responses. Completely drying alcoholic solvents is difficult, which explains why emission changes are observed in CH_3OH without the addition of exogenous water and why the absorption spectra of the oxidized FerriNaphth erodes slowly over time. Additional attempts to enhance the rate of the fluorescence response from FerriNaphth were unsuccessful. While the initial oxidation step is complete within minutes with stoichiometric Fe^{III}, the hydrolysis remains very slow even with the addition of catalytic water and acid. Evaluation of the emission intensity of FerriNaphth over time with Fe^{III} in the presence of water, CH_3COOH, H_3PO_4 and HNO_3 shows varying rates in the emission increase, although hydrolysis requires a period of several hours and remains incomplete even after several days. The slow fluorescence response of FerriNaphth and the incompatibility of naphthalimide fluorescence properties to aqueous conditions limit the potential biological application of this probe, but represent a unique signal transduction mechanism that could be adapted for such purposes.

In order to confirm the fluorescence signaling mechanism of FerriNaphth, we sought to confirm the identity of the quinone/imine-one tautomeric intermediate. In thoroughly dried CH_3CN, the peak at 368 nm corresponding to oxidized FerriNaphth remains stable for extended periods of time; however, only **7** can be isolated when the solvent is removed. The tautomeric species shows no appreciable fluorescence, which suggests the increase in emission intensity in the fluorescence studies can be attributed solely to **7**. Recently, a naphthalimide-based Zn^{2+} sensor has been reported that fluoresces at different wavelengths in its two tautomeric forms.[30] Since the intermediate remains stable in solution, tandem mass spectrometric (MS/MS) analysis was performed (Fig. 4). In addition to detecting a parent ion corresponding to a molecular weight of 2 mass units less than FerriNaphth, a fragmentation pattern consistent with the step-wise loss of two CO units was also observed. The combined experimental results suggest that catechol oxidation followed by a hydrolysis of a tautomeric quinone/imine-one correctly describes the mechanism of fluorescence enhancement.

To determine the extent of FerriNaphth's ability to detect metal oxidants, the probe was exposed to a variety of different oxidants at several different concentrations. $Cu(NO_3)_2$ oxidizes FerriNaphth, and the changes observed in the absorption spectra are similar to those measured using Fe^{III}. Oxidation of FerriNaphth using stoichiometric amounts of Cu^{II} proceeds at rates similar to Fe^{III} although Cu^{II} has a standard reduction potential that is ~0.6 V lower than Fe^{III}. Since the oxidation is relatively rapid, it is difficult to compare the rates of oxidation with the two metals with standard UV-vis instrumentation. Stopped flow techniques could elucidate more detailed kinetic information and may provide a methodology to discriminate between the two metal ions

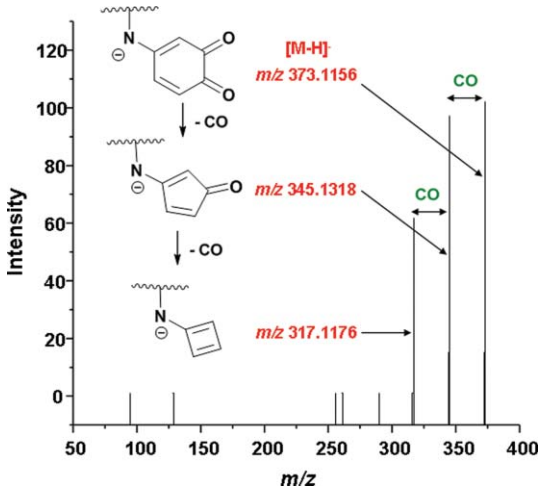

Fig. 4 MS/MS analysis of oxidized FerriNaphth. The parent quinone anion as well as peaks corresponding to the loss of CO units verify the identity of the oxidation product.

by rate analysis. In a manner analogous to the Fe^{III}/ferrozine assay, oxidation of FerriNaphth with Cu^{II} in the presence of neocuproine, a common indicator for Cu^{I}, results in a strong band at 480 nm that is indicative of $[Cu(neocuproine)]^{+}$ indicating approximately 2 equivalents of Cu^{II} are consumed in the oxidation (Fig. 3).

FerriNaphth does not oxidize in the presence of $AgNO_3$, which has a slightly more positive standard reduction potential than Fe^{III}, even at high concentrations of the metal ion. Ag^{I} does not coordinate strongly with catechol ligands like those in FerriNaphth, suggesting that coordination of the metal ion to ligand facilitates the oxidation. This conclusion is supported further by the results of assays using $Fe(CN)_6^{3-}$ and $[Co(NH_3)_5Cl]Cl_2$ as oxidants. Exposure of FerriNaphth to 10 or more equivalents of coordinatively saturated $Fe(CN)_6^{3-}$ shows no evidence of oxidation. FerriNaphth slowly oxidizes in the presence of $[Co(NH_3)_5Cl]Cl_2$ but the reaction remains incomplete after 48 h (Fig. 5). Even though Co^{III} is a strong oxidant, slow ligand exchange[31] with $[Co(NH_3)_5Cl]^{2+}$ results in decreased rates of oxidation. Unlike the other common oxidants screened, ceric ammonium nitrate causes the decomposition

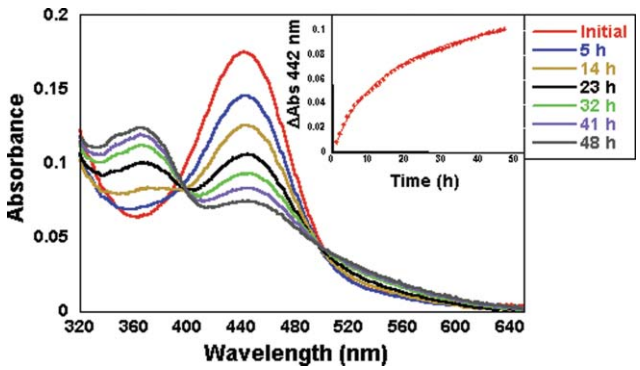

Fig. 5 Oxidation of 10 μM FerriNaphth with 6 equivalents of $[Co(NH_3)_5Cl]Cl_2$ in CH_3CN. The absorption spectra were automatically recorded every hour for 48 h. Inset: changes in the absolute value of the absorbance at 442 nm as a function of time.

of the probe into several unidentifiable fluorescent products suggesting FerriNaphth is incompatible with especially strong oxidants.

Since the rapid oxidation of FerriNaphth precludes examination of coordination chemistry, the redox inert structural analog of Fe^{III}, Ga^{III}, was employed for additional studies. In addition to coordination chemistry, Ga^{III} allows the examination of ICT states produced by metal ion binding when FerriNaphth is not oxidized. Titration of FerriNaphth with up to 20 equivalents of $Ga(NO_3)_3$ results in a slight red shifting (~7 nm) and a decrease in intensity of the absorption band centered at 441 nm and an increase in the absorption band at 360 nm. Ga^{III} titrations were carried out with the nitrate salt in MeOH because of limited solubility in CH_3CN; in addition, there are no readily available Ga^{III} salts that are compatible with the procedures used to assess FerriNaphth oxidation. When the FerriNaphth-Ga^{III} species is excited at 450 nm a modest 2-fold increase in the emission intensity can be measured (Fig. 6). The spectroscopic changes suggest Ga^{III} binds to the catechol of FerriNaphth generating an ICT state; however, the interaction does not appear to be very strong. At higher concentrations of $Ga(NO_3)_3$, evidence of FeriNaphth oxidation exists. Under acidic conditions, nitrate is a good oxidizing agent. Ga^{III} coordination to FerriNaphth lowers the pK_a of the coordinated phenols, which generates the conditions necessary for nitrate to act as an electron acceptor. Excess KNO_3 under acidic conditions also slowly oxidizes FerriNaphth. By adding additional acid to a solution containing FerriNaphth and 30 equivalents of $Ga(NO_3)_3$, the slow oxidation accelerates slightly. Fluorescence studies with Ga^{III} were carried out with 3 equivalents of Hunig's base to differentiate metal binding-based ICT states from ones resulting from oxidation. While some evidence of complexation between Ga^{III} and FerriNaphth was acquired, the persistence of oxidation reactions makes characterizing these weakly binding complexes difficult and ambiguous.

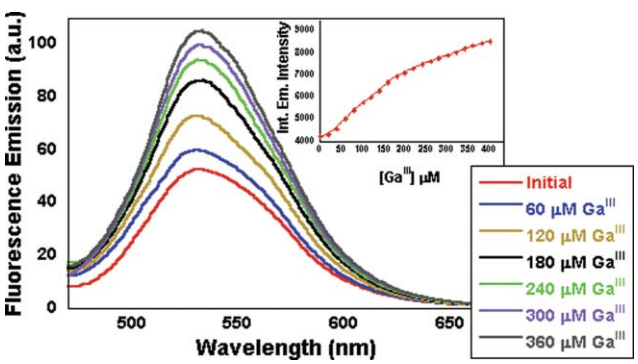

Fig. 6 Titration of 10 μM FerriNaphth in CH_3OH with $Ga(NO_3)_3$. Spectra were taken at 20 μM increments up to 360 μM of Ga^{3+}. Above 360 μM of $Ga(NO_3)_3$, nitrate mediated oxidation of FerriNaphth starts to occur. Each spectrum was corrected for dilution by multiplying the measured absorption and integrated emission intensity by the inverse of the dilution factor. The emission intensity was integrated from 470 to 650 nm. Excitation was provided at 450 nm with an excitation slit width of 5.0 nm and an emission slit width of 10.0 nm. Inset: changes in integrated fluorescence emission with increasing concentrations of Ga^{3+}.

Conclusions

In summary we have prepared and characterized a new fluorescent chemodosimeter for metal based oxidants based on a tandem oxidation–hydrolysis reaction of a catechol linked napthalimide dyad. FerriNaphth has a weak emission that increases significantly upon conversion into *N*-^{n}butyl-4-aminonaphthalimide in the presence of Fe^{III} and Cu^{II}. Non-coordinating metal oxidants and redox inactive metal ions have only a minimal effect on the absorption and emission properties of FerriNaphth. The absorption changes are similar to some recently described Cu^{II} sensors that possess similar aniline components and are deprotonated by metal ion coordination,[15] but additional studies are needed to make meaningful comparisons. The signaling mechanism has been confirmed by isolating the fluorescent species, detecting reduced Fe^{II} in the fluorescence assay, and characterizing the oxidized intermediate by mass spectroscopy. Future efforts will involve designing a chemodosimeter with an ICT mechanism by stabilizing the linkage between catechol and fluorophore to inhibit hydrolysis.

Experimental

Synthesis

General procedures. All materials listed below were of research grade or of spectrograde of highest purity available from TCI America or Acros Organics. Dichloromethane (CH_2Cl_2), toluene ($C_6H_5CH_3$) and tetrahydrofuran (THF) were sparged with argon and dried by passage through a Seca Solvent Purification System. Chromatography and TLC were performed on silica (230–400 mesh) obtained from Silicycle. TLCs were developed with mixtures of EtOAc/hexanes or CH_2Cl_2 unless otherwise stated. 4-Bromo-*N*-butyl-1,8-naphthalimide (**2**)[20] and 5-aminospiro(1,2-benzodioxole-2,1-cyclohexane) (**3**)[21] were prepared according to literature procedures. ^{1}H and ^{13}C were recorded using a Bruker 400 MHz NMR instrument. Chemical shifts are reported in ppm relative to tetramethylsilane. IR spectra were recorded on a Nicolet 205 FT-IR Instrument and the samples were prepared as KBr pellets. High resolution mass spectra were recorded at the University of Connecticut mass spectrometry facility using a micromass Q-Tof-2™ operating in positive mode.

2-Butyl-6-spiro (1,3-benzodioxole-2,1′-cyclohexane-phenylamino)-benzo[*de*]isoquinoline-1,3-dione (4). A Schlenk tube was charged with 600 mg (1.18 mmol) of **2**, 408 mg (2.0 mmol) of **3**, 26 mg of BINAP (2.3 mol%), 18 mg Pd (dba)$_3$, 480 mg (5.0 mmol) of sodium tertiary butoxide and toluene (100 mL). The process of freeze–pump–thaw was repeated and the tube was back-filled with nitrogen, then sealed and heated to 90 °C while stirring for 48 h. The mixture was filtered through Celite, followed by repeated washing of the residue with dichloromethane. Solvent was removed by reduced pressure to yield an orange-brown solid. Flash chromatography on silica using ethyl acetate–hexanes (4 : 1) yielded an orange solid. (775 mg, 58%). TLC R_f 0.25, 4/1 ethyl acetate–hexanes. ^{1}H NMR (400 MHz, $CDCl_3$) δ 8.47 (d, J = 7.2, 1 H), 8.41 (d, J = 8.4, 1 H), 8.27 (d, J = 8.52, 1 H), 7.7 (t, J = 7.52, 1 H), 7.1 (d, J = 8.6, 1 H), 6.80-6.72 (m, 4 H), 4.20 (t, J = 6.92, 2 H), 1.99-1.96 (m, 4 H), 1.78-1.69 (m, 6 H), 1.49-1.41 (m, 2 H), 1.29-1.25 (m, 1 H), m 1.01-0.96 (m, 3 H). ^{13}C NMR (100 MHz, $CDCl_3$) δ 164.8, 164.2, 184.8, 184.3, 145.9, 133.9, 132.8, 131.5, 130.1, 126.2, 125.4, 121.2, 117.10, 112.6, 108.8, 108.1, 106.1, 40.2, 35.4, 34.9, 35.4, 34.9, 30.5, 25.5, 24.7, 23.4, 20.6, 14.1. IR (thin film, cm^{-1}), 3349.2, 2935.9, 1684.79, 1640.91, 1581.7, 1535.4, 1429.5, 1390.4, 1360.99, 1344.6, 1240.7. HRMS (+ESI): Calcd. for M Na^+.479.1947; Found, 479.1993.

2-Butyl-6-(3,4-dihydroxy-phenylamino)-benzo[*de*]isoquinoline-1,3-dione (FerriNaphth, 1). Concentrated hydrochloric acid (16 mL) was added to a stirred suspension of **5** (300 mg, 0.65 mmol) in absolute ethanol (25 mL). The mixture was refluxed for 90 min followed by the removal of half of the solvent by vacuum. Water was added to precipitate a red solid. This was filtered and washed (2 × 5 mL) with water. The solid was collected and chromatographed on silica using 100% dichloromethane to yield a red crystalline solid (185 mg, 75%).TLC R_f 0.2, dichloromethane. ^{1}H NMR (400 MHz, DMSO) δ 9.18 (s, 2 H), 8.97 (s, 1 H), 8.82 (d, J = 8.7 Hz, 1 H), 8.48 (d, J = 7.1 Hz, 1 H), 8.22 (d, J = 8.3 Hz, 1 H), 7.76 (t, J = 8.0 Hz, 1 H), 6.96 (d, J = 8.5 Hz, 1 H), 6.84 (d, J = 8.2 Hz, 1 H), 6.78, (s, 1 H), 6.67 (d, J = 8.4 Hz, 1 H), 4.04 (t, J = 7.5 Hz, 2 H), 1.63 (sextet, J = 6.8 Hz, 2 H), 1.34 (septuplet, J = 7.4, 2 H), 0.94 (t, J = 7.2, 3 H). ^{13}C NMR (400 MHz, DMSO) δ 164.4, 163.5, 150.4, 146.7, 143.9, 134.4, 131.7, 131.6, 130.3, 129.5, 125.4, 122.6, 121.3, 116.7, 116.4, 113.29, 109.9, 107.1 IR (thin film, cm^{-1}), 3390.07, 3290.8, 2956.55, 2925.2, 1685.5, 1674.5 1638.3, 1612.1, 1580.5, 1565.4, 1542.1, 1530.1, 1520.6. HRMS (+ESI): Calcd. for M Na^+.399.1321; Found, 399.1352.

Spectroscopy

General methods. All solutions were prepared with spectrophotometric grade solvents. FerriNaphth was dissolved in DMSO to make a 10 mM stock solution. A 3 μL aliquot of FerriNaphth stock was placed in a quartz cuvette and diluted with 3 mL of CH_3CN to provide a 10 μM solution for spectroscopy unless otherwise noted. Stock solutions (10 mM) of each metal ion were prepared in 3/2 EtOH–CH_3CN unless otherwise noted. Absorption spectra were recorded on a Cary 50 UV-visible spectrophotometer operated by a PC equipped with Pentium-IV processor. Spectra were taken at 25 °C in 1-cm path length cuvettes. Fluorescence spectra were recorded on a Hitachi F-4500 spectrophotometer operated by a PC equipped with a Pentium-IV processor, running the FL solutions 2.0 software. A 150 W Xe lamp operating at 5 A provided excitation. Spectra were acquired in a quartz cuvette with a 1-cm path length. Slit widths are 5 nm for excitation and 10 nm for emission with a photomultiplier tube voltage of 700 V, unless stated otherwise.

UV-Vis experiments with $Cu(NO_3)_2$ and $Fe(NO_3)_3$. The initial spectrum of 10 mM FerriNaphth solution was recorded. Metal ion stock was added incrementally up to 21.6 μM and spectra were recorded after equilibrium was reached following each addition (~ 5 min). Experiments in MeOH were performed using identical procedures.

UV-Vis experiments with $K_3Fe(CN)_6$, $AgNO_3$ and $[Co(NH)_5Cl]Cl_2$. For $K_3Fe(CN)_6$ and $AgNO_3$, the initial spectrum of a 10 μM solution of FerriNaphth was recorded which was followed by the addition of a 2 equivalents of the metal complex. The spectra were monitored for changes over a period of 20 min. An additional 8 equivalents of metal complex was added to the cuvette and spectra were monitored for an additional 10 min. The experiment was repeated using a 1.71 mM stock solution of $[Co(NH)_5Cl]Cl_2$ which was prepared in 2/1/1 MeOH–DMSO–H_2O. The initial spectrum of a 10 μM solution of FerriNaphth was recorded followed by the addition of a 6-fold excess of metal. Spectra were recorded every hour for 48 h.

UV-Vis experiments with ferrozine and neocuproine. Commercially available ferrozine indicator was dissolved in a 4/1 MeOH–H_2O to make 10 mM stock solutions. A 1 mM stock solution of $Fe(NO_3)_3$ was prepared in 9/1 CH_3CN–EtOH. Solutions were prepared by mixing 10 μM of FerriNaphth in CH_3CN with a 10-fold excess of both indicator and metal ion. The mixture was allowed to equilibrate for 0.5 h and the spectrum was recorded. Commercially available Neocuproine indicator was dissolved in CH_3CN to make a 10 mM solution, and analogous procedures to the ferrozine assay were utilized for the neocuproine experiment except a 20-fold excess of indicator was used.

Emission studies with $Fe(NO_3)_3$. Spectra of 10 μM FerriNaphth in CH_3CN was recorded before and after oxidation with $Fe(NO_3)_3$. After the addition of 30 μL of H_2O, an emission spectrum was recorded every 8 min for 48 min. The excitation wavelength was $\lambda_{ex} = 400$ nm. The excitation slit width was 5 nm and emission 10 nm.

Emission studies with $Ga(NO_3)_3$. Stock solution of 10 mM $Ga(NO_3)_3$ was prepared in a 9/1 MeOH–DMSO. The initial emission spectrum of a 10 μM solution of FerriNaphth in MeOH was recorded followed by the addition of metal in 20 μM increments. Spectra were recorded after each addition. The excitation wavelength was $\lambda_{ex} = 450$ nm. The excitation slit width was 5 nm and emission 10 nm. The area under the emission spectra was integrated between 470–650 nm. The absorption spectra were recorded after the addition of each 20 μM increment of metal.

Quantum yield. Quantum yields were calculated by measuring the integrated emission area of the corrected spectra and comparing that value to the area measured for Quinine in 0.5 M H_2SO_4 when excited at 365 nm ($\Phi_{fl} = 0.54$).[32] The quantum yields for FerriNaphth were calculated using eqn (1), where F represents the area under the emission spectra for the standard samples, η is the refractive index of the solvent and Abs is the absorbance at the excitation wavelength selected for the standard and samples. Emission spectra were integrated between 440–640 nm (λ_{ex} = 400 nm, 10^{-6} M/$abs_{400} \sim 0.1$).

$$\Phi_{fl}^{sample} = \Phi_{fl}^{standard}\left(\frac{F^{sample}}{F^{standard}}\right)\left(\frac{\eta^{sample}}{\eta^{standard}}\right)\left(\frac{Abs^{standard}}{Abs^{sample}}\right) \quad (1)$$

Mass spectroscopy. Tandem mass spectrometric (MS/MS) analysis was performed on a quadrupole-time-of-flight tandem mass spectrometer (QTOFmicro, Waters, Milford, MA), equipped with an in-house modified electrospray (ESI) source. The compound was dissolved in CH_3CN, and diluted with 10 mM ammonium bicarbonate in CH_3CN–H_2O (1 : 1, v/v). The sample solution was infused to a mass spectrometer with a flow rate of 50 μL min^{-1}. Key instrument parameters for the mass spectrometer, run under negative ion mode, were as follows: capillary voltage 2800 V, cone voltage (CV) 15 V, extraction voltage 2 V, collision energy (CE) offset 25 V. The MS/MS spectrum was obtained by selecting the negatively charged molecular ion ($[M - H]^-$, m/z 373.1) as precursor. The proposed fragmentation mechanism (loss of CO) was based on the accurate mass measurement.

Notes and references

1 P. Jiang and Z. Guo, *Coord. Chem. Rev.*, 2004, **248**, 205–229.
2 R. Y. Tsien, *Annu. Rev. Neurosci.*, 1989, **12**, 227–253.
3 J. L. Bricks, A. Kovalchuk, C. Trieflinger, M. Nofz, M. Buschel, A. I. Tolmachev, J. Daub and K. Rurack, *J. Am. Chem. Soc.*, 2005, **127**, 13522–13529.
4 E. L. Que, D. W. Domaille and C. J. Chang, *Chem. Rev.*, 2008, **108**, 1517–1549.
5 D. P. Kennedy, C. M. Kormos and S. C. Burdette, *J. Am. Chem. Soc.*, 2009, **131**, 8578–8586.
6 A. C. Benniston, G. Copley, K. J. Elliott, R. W. Harrington and W. Clegg, *Eur. J. Org. Chem.*, 2008, 2705–2713.
7 Z. N. Sun, F. Q. Liu, Y. Chen, P. K. H. Tam and D. Yang, *Org. Lett.*, 2008, **10**, 2171–2174.
8 Z. N. Sun, H. L. Wang, F. Q. Liu, Y. Chen, P. K. H. Tam and D. Yang, *Org. Lett.*, 2009, **11**, 1887–1890.
9 R. Kikkeri, H. Traboulsi, N. Humbert, E. Gumienna-Kontecka, R. Arad-Yellin, G. Melman, M. Elhabiri, A. M. Albrecht-Gary and A. Shanzer, *Inorg. Chem.*, 2007, **46**, 2485–2497.
10 N. C. Lim, S. V. Pavlova and C. Bruckner, *Inorg. Chem.*, 2009, **48**, 1173–1182.
11 Y. Xiang and A. J. Tong, *Org. Lett.*, 2006, **8**, 1549–1552.
12 V. Dujols, F. Ford and A. W. Czarnik, *J. Am. Chem. Soc.*, 1997, **119**, 7386–7387.
13 L. M. Hyman, C. J. Stephenson, M. G. Dickens, K. D. Shimizu and K. J. Franz, *Dalton Trans.*, 2010, 568–576.
14 H. N. Kim, M. H. Lee, H. J. Kim, J. S. Kim and J. Yoon, *Chem. Soc. Rev.*, 2008, **37**, 1465–1472.
15 J. H. Huang, Y. F. Xu and X. H. Qian, *Dalton Trans.*, 2009, 1761–1766.
16 J. H. Huang, Y. F. Xu and X. H. Qian, *Org. Biomol. Chem.*, 2009, **7**, 1299–1303.
17 Z. C. Xu, Y. Xiao, X. H. Qian, J. N. Cui and D. W. Cui, *Org. Lett.*, 2005, **7**, 889–892.
18 Z. C. Xu, X. H. Qian and J. N. Cui, *Org. Lett.*, 2005, **7**, 3029–3032.
19 S. Saha and A. Samanta, *J. Phys. Chem. A*, 2002, **106**, 4763–4771.
20 B. Liu and H. Tian, *Chem. Commun.*, 2005, 3156–3158.
21 R. L. Clark, A. A. Pessolano, T.-Y. Shen, D. P. Jacobus, H. Jones, V. J. Lotti and L. M. Flataker, *J. Med. Chem.*, 1978, **21**, 965–978.
22 D. Srikun, E. W. Miller, D. W. Dornaille and C. J. Chang, *J. Am. Chem. Soc.*, 2008, **130**, 4596–4597.
23 M. S. Alexiou, V. Tychopoulos, S. Ghorbanian, J. H. P. Tyman, R. G. Brown and P. I. Brittain, *J. Chem. Soc., Perkin Trans. 2*, 1990, 837–842.
24 D. J. Liberato, V. S. Byers, R. G. Dennick and N. C. Jr, *J. Med. Chem.*, 1981, **24**, 28–33.
25 R. Ohshima, M. Kitamura, A. Morita, M. Shiro, Y. Yamada, M. Ikekita, E. Kimura and S. Aoki, *Inorg. Chem.*, 2010, **49**, 888–889.
26 W. Y. Lin, L. Yuan, J. B. Feng and X. W. Cao, *Eur. J. Org. Chem.*, 2008, 2689–2692.

27 S. Aoki, K. Sakurama, R. Ohshima, N. Matsuo, Y. Yamada, R. Takasawa, S. I. Tanuma, K. Talkeda and E. Kimura, *Inorg. Chem.*, 2008, **47**, 2747–2754.
28 X. Qi, E. J. Jun, L. Xu, S. J. Kim, J. S. J. Hong, Y. J. Yoon and J. Y. Yoon, *J. Org. Chem.*, 2006, **71**, 2881–2884.
29 A. Mokhir and R. Kramer, *Chem. Commun.*, 2005, 2244–2246.
30 Z. Xu, K.-H. Baek, H. N. Kim, J. Cui, X. Qian, D. R. Spring, I. Shin and J. Yoon, *J. Am. Chem. Soc.*, 2010, **132**, ASAP.
31 H. Diebler, M. Eigen, G. Ilgenfritz, G. Maass and R. Winkler, *Pure Appl. Chem.*, 1969, **20**, 93–115.
32 G. A. Crosby and J. N. Demas, *J. Phys. Chem.*, 1971, **75**, 991–1024.